A Possible Cooperative Structural Transition of DNA in the 0.25–2.0 pN Range

ARTICLE *in* THE JOURNAL OF PHYSICAL CHEMISTRY B · MAY 2015

Impact Factor: 3.3 · DOI: 10.1021/acs.jpcb.5b03174 · Source: PubMed

1 AUTHOR:

J. Michael Schurr

University of Washington Seattle

178 PUBLICATIONS **4,100** CITATIONS

THE JOURNAL OF PHYSICAL CHEMISTRY B

Article

pubs.acs.org/JPCB

A Possible Cooperative Structural Transition of DNA in the 0.25−2.0 pN Range

J. Michael Schurr*

Department of Chemistry, University of Washington, Box 351700, Seattle, Washington 98195, United States

ABSTRACT: The measured *effective* torsional rigidities of single twisted DNAs under various tensions conflict with theoretical predictions of Moroz and Nelson (MN) at low forces in the 0.25−2.0 pN range. However, MN theory was recently shown to agree well with effective torsional rigidities obtained from simulations, indicating that MN theory is valid down to 0.25 pN for a filament with a constant *intrinsic* torsional rigidity. Here MN theory is used with an assumed persistence length, 50 nm, to obtain the *force-dependent intrinsic* torsional rigidity of the filament at each force from its measured *effective* torsional rigidity. The resulting values rise ∼1.8-fold with increasing force from 0.25 to 2.0 pN. Unexpected behavior of the relative extensions of the *untwisted* DNAs of Mosconi et al. is noted, and ascribed to a small increase in contour length with force over the 0.18−2.0 pN range. The variations of both the intrinsic torsional rigidity and rise per base pair (bp) with force are suggested to arise from a force-induced shift of a cooperative equilibrium between two conformations with different rises per bp. A two-state nearest-neighbor model is formulated, and ranges of optimal parameters are determined by fitting the model to the experimental differences in rise per bp as a function of force. Optimal adjustment of the torsion elastic constants of the two states enables the same optimal model(s) with fixed parameters to provide reasonably good fits of the experimental torsion elastic constant data. The results reconcile single-molecule measurements on DNAs under tension with numerous results from fluorescence polarization anisotropy, topoisomer distributions, X-ray scattering of DNAs with attached gold colloids, and other kinds of measurements.

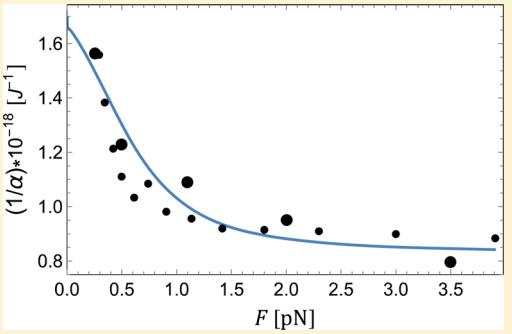

INTRODUCTION

Conflict between theory and experiment often leads to new insights and revision of current paradigms. The relevant conflict addressed here is between the theory of Moroz and Nelson[1,2] and the experimental data of Mosconi et al.[3] and Lipfert et al.[4] pertaining to single twisted DNA molecules under tension. The proposed resolution of this conflict contradicts two common, though not universally held, beliefs: (1) duplex DNAs in solution do not exhibit highly cooperative fluctuations between nearly iso-free-energetic states with different mechanical properties, and (2) pulling forces less than 5.0 pN are too weak to induce significant changes in the intrinsic structural and mechanical properties of DNA, such as its rise per base pair (bp) and torsional rigidity. Other kinds of evidence that contradict these two prevailing dogmas, and their relation to long-range cooperative allosteric transitions induced by the binding of proteins and other ligands, are discussed after the analysis is completed.

Moroz and Nelson (MN) developed a theory for the relative extension and torque of a single wormlike filament with uniform intrinsic flexural (bending) and torsional (twisting) rigidities as a function of both pulling force and the number of excess incorporated turns.[1,2] This theory applies only under conditions of sufficiently high force and low twist (or equivalently low superhelix density) that self-interactions of the filament make no significant contribution. An analytical expression relating the torque to the intrinsic torsional and bending rigidities, tension, and superhelix density of the filament was derived. The *effective* torsional rigidity, C^{eff}, which typically lies below the intrinsic value, C^{in} (due to conversion of some of the imposed twist into writhe), was obtained simply as the slope of the torque with respect to the imposed twist. Another analytical expression relating the relative extension to the bending rigidity, force, and torque was also obtained. These two analytical expressions were obtained via expansions about the high force limit.

Experimental measurements[3,4] of the torques of single DNAs in ∼0.1 M ionic strength solutions at ambient temperature under various constant tensions from 0.25 to 6.5 pN as a function of excess twist were obtained by two different technical *tours de force*. These data enabled a determination of the effective torsional rigidities *in the small-twist limit*. Mosconi et al.[3] measured remarkably precise curves of relative extension vs superhelix density at various constant forces from 0.13 to 3.9 pN. The torques were ascertained by using a thermodynamic Maxwell relation and numerically integrating over the relevant paths. From the limiting slope of the torque with respect to twist, the *effective* torsional rigidity of the filament *in the limit of small twist* was obtained for each force from 0.29 to 3.9 pN by this so-called indirect method. Lipfert et al.[4] measured directly the effective torque of a single twisted DNA molecule at various forces from 0.25 to 6.5 pN by means

Received: April 1, 2015
Revised: April 29, 2015

DOI: 10.1021/acs.jpcb.5b03174
J. Phys. Chem. B XXXX, XXX, XXX−XXX

of a magnetic torque tweezers method. Both groups compared their small-twist effective torsional rigidities at different tensions with predictions of the MN theory. When the *intrinsic* torsional rigidity, C^{in}, was chosen so that the MN theory yielded an effective torsional rigidity, C^{eff}, equal to or near the experimental value at the highest force (i.e., 3.9 pN for Mosconi et al. and 6.5 pN for Lipfert et al.), the experimental C^{eff} values at successively lower forces fell increasingly farther below the predictions of MN theory *with the same value of* C^{in}. For the data of Mosconi et al., the value of C^{eff} at F = 0.29 pN was ∼0.56-fold smaller than the MN prediction. For the data of Lipfert et al., which exhibited a somewhat greater value of C^{eff} at both 3.5 and 6.5 pN, from which a somewhat greater value of C^{in} was inferred, the value of C^{eff} at F = 0.25 pN was 0.55-fold smaller than its corresponding MN prediction.

These large (∼1.8-fold) discrepancies between MN theory with a single rather high value of the intrinsic torsional rigidity, typical of values obtained at higher forces,[5] and the measured C^{eff} values at the lowest forces (0.25 or 0.29 pN) admit several possible interpretations: (1) The MN theory is invalid at such low forces, due to inaccuracy of the expansion about the high force limit, and/or inaccuracy associated with the use of the Fuller write, and/or the effects of self-interactions of the filament, which are neglected in MN theory, and/or other errors in the theory. (2) MN theory is substantially correct in the small-twist limit for all forces down to F = 0.25 pN, but the intrinsic torsional rigidity, C^{in}, is not constant and instead varies with pulling force in the low-force regime, especially between 0.25 and 2.0 pN. (3) The experimental values of C^{eff} at low forces are all erroneous. Possibility (3) is discounted here for various reasons, including the approximate agreement between the results of Mosconi et al. and Lipfert et al., who employed very different methods. Also, a comparably large decrease in C^{eff} with decreasing force was observed for a considerably shorter (3.4 kbp) DNA by a freely orbiting magnetic tweezers method that measures fluctuations in twist of a torsionally unconstrained DNA.[6] (These latter data are not treated here, because the 0.35 μm radius of the magnetic bead is 30% of the length of that shorter DNA, raising the possibility that in some cases the orientation of a significant fraction of the DNA might be influenced by its proximity to the bead.) Possibility (2) was proposed in prior work[7] but was not discussed by either experimental group. Possibility (1) is implicit in the discourses of both Mosconi et al. and Lipfert et al. Both groups noted the use of a high force expansion in MN theory, and Lipfert et al. suggested that at least some of the discrepancy between the theory and experiment is likely attributable to inaccuracies associated with that. The language of both groups makes clear their belief that there is only a single value of the intrinsic (bare) torsional rigidity, which corresponds to the limiting value of C^{eff} at high forces. *If* C^{in} *is actually a constant, independent of force*, as was presumed, then one is forced to conclude that MN theory is invalid at the lower forces, and possibility (1) necessarily prevails.

Both groups also noted that the experimental values of C^{eff} at the lowest forces (F = 0.25−0.29 pN) fall in the range of torsional rigidities obtained for unstrained DNAs by time-resolved fluorescence polarization anisotropy (FPA) of intercalated dyes,[8−15] thereby suggesting that the FPA method yields C^{eff} rather than the intrinsic torsional rigidity, C^{in}. However, an earlier Brownian dynamics study[16] showed that, for a linear 196 bp DNA free in solution, the FPA method recovers a best-fit value of C that only slightly (by 0.92- to 0.95-fold) underestimates the known input value of the *intrinsic* torsional rigidity. Another prior study[7] compared measured supercoiling free energies of *weakly strained* superhelical circular DNAs with results of Monte Carlo reversible work simulations of the supercoiling free energies for different trial values of the *intrinsic* torsional rigidity. Intrinsic torsional rigidities in the range 170 fJ fm ≤ C^{in} ≤ 230 fJ fm, typical of FPA measurements, were compatible with the experimental supercoiling free energies, whereas those in the range C^{in} ≥ 269 fJ fm, which encompasses all previously reported values for DNAs under tension, were not. These two studies contradict any notion that the intrinsic torsional rigidities of unstrained or only weakly strained DNAs are comparable to the much greater intrinsic torsional rigidities that prevail at high forces, F ≥ 4.0 pN, which typically lie in the range 380−420 fJ fm.

A primary objective here is to examine the alternative interpretation (2) above, according to which MN theory is valid (sufficiently accurate) over the range of forces considered here, but the intrinsic torsional rigidity varies with the pulling force.

VALIDITY OF MOROZ−NELSON THEORY

Moroz and Nelson provided a criterion for validity (acceptable accuracy) of their high force expansion.[1,2] *In the small-twist limit*, where the torque is negligibly small, this criterion is $K^2 \equiv PF/kT \geq 2.0$, where K^{-1} is the expansion parameter, P is the bending persistence length, F is the pulling force, and kT is the thermal energy. For the lowest forces considered here, namely, F = 0.25 and 0.29 pN, and a consensus persistence length, P = 50 nm, one has, respectively, K^2 = 3.09 and 3.58, so this criterion is easily met for those and all higher forces *in the small-twist limit*.

A recent study of Chou et al.[17] carefully examined possible sources of error in modeling DNA and RNA tweezers experiments by performing Monte Carlo simulations of coarse-grained base-pair-level models with step-parameter distributions derived from X-ray crystal structures. Such models can be regarded as discretized and elaborated versions of the wormlike coil model, whose elastic properties averaged over sufficient length should be comparable to those of a wormlike coil model with the appropriate intrinsic elastic constants. Chou et al. investigated a number of potential problems and artifacts, including the domain of validity of the Fuller writhe, which is used in MN theory, the effects of tethering constraints, and the occurrence of self-interactions (steric clashes). The Fuller writhe was found to be "effectively exact" for all forces exceeding 0.4 pN, and even at 0.1 pN, it failed only for superhelix density, $\sigma \geq 0.022$. Since the experimental measurements of C^{eff} in the small-twist limit involve only data for $\sigma \leq 0.01$, the use of the Fuller writhe formula should introduce negligible error for all $F \geq 0.25$ pN. The effects of tethering constraints were found to be negligibly small, and zero steric clashes were observed in 1000 independent configurations of a 3000 bp model DNA at F = 0.4 pN. Most importantly, the MN formula for C^{eff} gave a good fit to the simulated C^{eff} values as a function of force over the range F = 0.25−4.0 pN, with a maximum relative deviation of less than ∼4% (due primarily to statistical errors in the simulations). Moreover, the best-fit value of the intrinsic torsional rigidity, C^{in}, matched the limiting (high force) value of C^{eff}. All C^{eff} values were reckoned from the variance of the fluctuating linking number in simulations of torsionally unconstrained filaments. These results indicate that MN theory for C^{eff} is at least moderately accurate, and possibly very accurate, for a

DOI: 10.1021/acs.jpcb.5b03174
J. Phys. Chem. B XXXX, XXX, XXX−XXX

Table 1. Experimental Data of Mosconi et al.[3] and Lipfert et al.[4]

F (pN)	C_{mos}^{eff} [a] (fJ fm)	C_{lip}^{eff} [b] (fJ fm)	C_{MN}^{in} [c] (fJ fm)	$(z_F/z_{max})_0$ [d]	P_{app} [e] (nm)	$L_F/L_{3.9}$ [f]	$\alpha_{MN} \times 10^{19}$ [g] (J)
0.18				0.63	41.8	0.932	
0.25		178 ± 8	216	0.685	41.2	0.940	6.39
0.29	182 ± 18		217	0.71	41.9	0.947	6.42
0.35	205 ± 18		244	0.735	41.5	0.949	7.22
0.42	233 ± 32		278	0.755	40.4	0.949	8.22
0.50	256 ± 26	235 ± 8	305, 275 (lip)	0.78	42.1	0.957	9.02, 8.14
0.61	278 ± 1		328	0.80	41.7	0.959	9.70
0.74	270 ± 22		311	0.826	45.3	0.970	9.20
0.91	299 ± 16		344	0.85	49.5	0.979	10.18
1.10		277 ± 8	310				9.17
1.13	311 ± 4		353	0.87	53.1	0.984	10.44
1.42	327 ± 22		367	0.89	59.0	0.990	10.86
1.80	334 ± 24		370	0.905	62.3	0.992	10.95
2.0		324 ± 8	356				10.53
2.3	340 ± 15		372	0.920	68.8	0.995	11.01
3.0	347 ± 39		376	0.934	77.5	0.997	11.12
3.5		392 ± 8	426				12.60
3.9	357 ± 49		383	0.947	92.4	1.000	11.33

[a]Effective torsional rigidity reported by Mosconi et al.[3] [b]Effective torsional rigidity reported by Lipfert et al.[4] [c]Force-dependent intrinsic torsional rigidity obtained from C_{mos}^{eff} or C_{lip}^{eff} by using MN theory in eq 1 with $\sigma = 0.001$ to enforce the small-twist limit. [d]Relative extension *at zero twist* data of Mosconi et al.,[3] where z_{max} is the (unknown) best-fit contour length of a wormlike-coil model fitted to extension (z_F) vs force (F) data for the untwisted DNA over a wide range of forces. [e]*Apparent* persistence length obtained from the relative extension data of Mosconi et al.[3] for DNAs *with zero twist* by applying the MN eq 2 under the assumption that the contour length remains constant at z_{max} independent of the force. [f]Ratio of apparent force-dependent contour length (L_F) at force F to that at 3.9 pN, which is obtained by applying eq 4, based on the MN eq 3, under the assumption that the persistence length remains fixed at the consensus value, $P = 50$ nm, independent of the force. [g]Force-dependent intrinsic torsion elastic constant of the effective springs between bp's obtained from C_{MN}^{in} according to $\alpha_{MN} = C_{MN}^{in}/h_0$, where $h_0 = 0.338$ nm is the consensus rise per bp.

filament in the small-twist regime, $\sigma \leq 0.01$, for all forces from $F = 4.0$ down to $F = 0.25$ pN! Hence, the large discrepancy between experimental and predicted values of C^{eff} most likely arises *not* from some failure of MN theory but instead from some variation of the intrinsic torsional rigidity, C^{in}, with tension.

PLAN OF THE PAPER

In the following section, MN theory is assumed to be correct, and is used to estimate the force-dependent intrinsic torsional rigidity, C_{MN}^{in}, from the corresponding experimental value of C^{eff} at that same force, and an assumed persistence length, $P = 50$ nm. The variation of C_{MN}^{in} with F suggests the possible involvement of a saturable structural transition.

In subsequent sections, unexpected behavior of the *relative extensions at zero twist* of Mosconi et al. as a function of the pulling force is tentatively ascribed to a slight variation in contour length with force. This in turn is attributed to force-induced shifting of the equilibrium position of a cooperative transition between two structural conformers, labeled a and b, that differ slightly in contour length. Such a transition was originally proposed by Mathew-Fenn et al.[18] and Shi et al.[19] to account for a significant largely all-or-none contribution to length fluctuations manifested in their X-ray scattering experiments on short (10−35 bp) DNAs with attached gold colloids. Fitting such a pulled equilibrium model to the differences in contour length (or rise per bp) at various forces does not yield a unique best-fit solution but does provide a range of differences in length between the two states and a range of corresponding cooperativity parameters that yield acceptable fits. The fractions, f_a and f_b, of bp's in each of the two states are reckoned at each force using a particular choice of the fitted parameters. Then, the torsion elastic constants, α_a and α_b, of the effective springs between bp's in the two states are adjusted to give an acceptable, though again not unique, fit of the theoretical inverse force-dependent intrinsic torsion elastic constants, $\langle 1/\alpha_F^{th} \rangle = (f_a/\alpha_a) + (f_b/\alpha_b)$, to the corresponding experimental values, $1/\alpha_{MN} = (C_{MN}^{in}/h_0)^{-1}$, where $h_0 = 0.338$ nm is the consensus rise per bp. A plausible, but again nonunique, fit is obtained with the estimated values, $\alpha_b = (11.95-12.05) \times 10^{-19}$ J and $\alpha_a = (5.44-4.13) \times 10^{-19}$ J, for the longer and shorter conformers, respectively.

In principle, such a cooperative two-state model could (1) account for the variation of intrinsic torsion elastic constants (and torsional rigidities) with applied force; (2) reconcile the intrinsic torsional rigidities obtained from single-molecule torque measurements at various forces with those obtained for unstrained or only weakly strained DNA by either FPA or comparison of experimental and simulated supercoiling free energies; (3) account for the cooperative fluctuations in DNA length reported by Mathew-Fenn et al.[18] and Shi et al.;[19] and (4) account for some of the long-range allosteric transitions induced by various local perturbations, including site-specific protein binding.[14]

ANALYSIS OF REPORTED EXPERIMENTAL DATA

Determination of C^{in} from Measured C^{eff}. The experimental forces, F, and effective torsional rigidities, C^{eff}, in the small-twist limit reported by Mosconi et al.[3] or Lipfert et al.[4] are listed under C_{mos}^{eff} and C_{lip}^{eff}, respectively, in Table 1.

The full MN expression[2] for C^{eff}/kT is

DOI: 10.1021/acs.jpcb.5b03174
J. Phys. Chem. B XXXX, XXX, XXX−XXX

$$C^{\mathrm{eff}}/kT = 1/(\mathrm{kT}/C^{\mathrm{in}}_{\mathrm{MN}} + (1/4PK)(1 + 1/(2K) + 21/(64K^2) + ((\tau/kT)^2/(16K^3))(2 + 15/(8K) + 9/(8K^2)) + ((\tau/kT)^2/(16K^3))(9/4)(5 + 15/K + 112/(9K^2)))) \quad (1)$$

wherein the torque divided by kT is given by $\tau \equiv (C^{\mathrm{eff}}/kT)\omega_0\sigma$, where $\omega_0 = 2\pi/((10.50)h_0) = 1.77 \times 10^9$ rad/m, $h_0 = 0.338$ nm is the consensus rise per bp, and σ is the superhelix density, which is here chosen to be 0.001 to enforce the small-twist limit; $P = 50$ nm is the *assumed* persistence length in ~100 mM ionic strength; $K \equiv (PF/kT - \tau^2/4)^{1/2}$ is the inverse expansion parameter, and $kT = 4.0463 \times 10^{-21}$ J at 293 K. For each experimental value of F and C^{eff} in Table 1, the intrinsic torsional rigidity, $C^{\mathrm{in}}_{\mathrm{MN}}$, is obtained by numerically solving eq 1. The resulting values are listed in Table 1.

For reasons described later, the $C^{\mathrm{in}}_{\mathrm{MN}}$ values in Table 1 are converted to torsion elastic constants of the effective springs between bp's, $\alpha_{\mathrm{MN}} = C^{\mathrm{in}}_{\mathrm{MN}}/h_0$, which are also listed in Table 1, and the reciprocals of which are plotted in Figure 1.

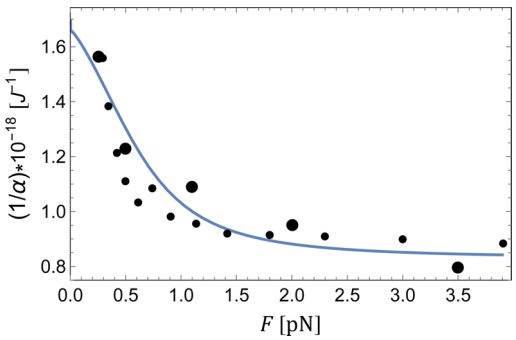

Figure 1. Inverse *intrinsic* torsion elastic constant $(1/\alpha)$ of the effective springs between bp's vs pulling force (F). Black dots are experimental points $(1/\alpha_{\mathrm{MN}})$, which were derived from the *effective* torsional rigidities at small twist reported by Mosconi et al.[3] (small dots) and Lipfert et al.[4] (large dots) by applying the Moroz–Nelson theory in eq 1. The solid curve is $\langle 1/\alpha_F^{\mathrm{th}} \rangle$ predicted by eq 12 for the two-state nearest-neighbor model with the same parameters as in Figure 2 and "optimal" values of the torsion elastic constants assigned to the *a* and *b* states, $\alpha_a = 4.81 \times 10^{-19}$ J and $\alpha_b = 12.05 \times 10^{-19}$ J, as described in the text. The standard deviation, $\sigma_{1/\alpha_{\mathrm{MN}}} = 1 \times 10^{17}$ J^{-1}, was estimated semiquantitatively from the deviations of $1/\alpha_{\mathrm{MN}}$ from this smooth curve through the data.

The variation of $1/\alpha_{\mathrm{MN}}$ with F and its apparent "saturation" at large F are plainly apparent. The origin of the smooth curve will be described later. The values of $C^{\mathrm{in}}_{\mathrm{MN}}$ at $F = 0.25$ and 0.29 pN lie within the typical range from FPA measurements (160–230 fJ fm), whereas, in the range $F = 3.0$–3.9 pN, they lie within the range 350–450 fJ fm obtained in other single-molecule pulling experiments at forces $F \geq 3.0$ pN.

The present situation resembles a previous circumstance involving small circular DNAs with $N \leq 254$ bp's, for which torsional rigidities were estimated by topoisomer ratio methods.[20,21] The resulting values substantially (by ~1.5–2.0-fold) exceeded those obtained by FPA for unstrained or only weakly strained DNAs. However, subsequent FPA studies of both linear and circular forms of the same 181 bp DNA demonstrated that the coherent bending strain imposed by circularization caused an ~1.5-fold immediate increase in torsion elastic constant, which over time increased further to a value that was ~1.8-fold greater than the age-invariant value of its corresponding linear DNA.[13] The immediate and delayed values for the circles corresponded closely to those extracted from topoisomer ratio data reported by, respectively, Horowitz and Wang[20] on one hand and Shore and Baldwin,[21] after correction,[22] on the other. The conclusion that sufficient bending strain alters the torsional rigidity was affirmed by cyclization kinetics studies of significantly larger, and therefore less strained, DNAs containing $N = 340$–350 bp's, which yielded a torsional rigidity typical of FPA measurements on unstrained DNAs.[23]

In the case of a DNA under tension, is there other evidence, such as a change in contour length, for a structural transition in the $F = 0.25$–3.9 pN range?

Analysis of Relative Extension vs Force Data for Untwisted DNAs. For a DNA subject to a force F and arbitrary imposed net twist, Moroz and Nelson derived an expression for the relative extension, z_F/z_{max}, where z_F is the measured extension and z_{max} is the contour length of the DNA. The experimental value of z_{max} is typically obtained by fitting MN or another accurate theory to measured z_F vs F data for DNA *at zero twist*. Moroz and Nelson gave an expansion of z_F/z_{max} in terms of $1/K$, similar to that in eq 1, but also presented a much simpler approximate relation that is extremely accurate *for the case of zero incorporated twist* over the range of forces considered here, namely,

$$z_F/z_{\mathrm{max}} = (1 - (0.5)/(PF/kT - 1/32)^{1/2}) \quad (2)$$

For a sufficiently long DNA *at zero twist*, the model of Moroz and Nelson[1,2] should exhibit the same relative extension as that of Marko and Siggia,[24] who treated an inextensible wormlike coil in the absence of any torsional constraints. Those authors formulated a "numerically exact" (to eight-digit accuracy) solution as an algorithm involving the lowest eigenvalue of a 101 × 101 force-dependent matrix (for $l = 0$–100, where l is a Legendre polynomial rank). In the present study, the ratio of the relative extension $(z_F/z_{\mathrm{max}})_{\mathrm{MN}}$, computed using eq 2, to the numerically exact value $(z_F/z_{\mathrm{max}})_{\mathrm{MS}}$, computed according to the Marko–Siggia algorithm, was reckoned for $F = 0.25$, 0.42, 0.74, 1.13, and 3.9 pN, and the respective ratios obtained were $(z_F/z_{\mathrm{max}})_{\mathrm{MN}}/(z_F/z_{\mathrm{max}})_{\mathrm{MS}} = 1.001856$, 1.000455, 1.00012, 1.000041, and 1.000001. Even in the worst case, $F = 0.25$ pN, these deviations from 1.0 are negligibly small, so eq 2 is practically exact over this range of forces.

The values of $(z_F/z_{\mathrm{max}})_0$ at zero twist that were reported by Mosconi et al.[3] are listed in Table 1. First, the apparent persistence lengths, P_{app}, for each force were reckoned from the corresponding $(z_F/z_{\mathrm{max}})_0$ at each force by using eq 2, and the resulting values are also listed in Table 1. At low forces from 0.18 to 0.61 pN, the P_{app} values lie significantly below the consensus range, $P = 50 \pm 2$ nm, for DNAs in ~0.1 M ionic strength of univalent ions.[25−28] With increasing force from 0.74 to 1.13 pN, P_{app} rises systematically to pass through the consensus range. P_{app} continues to rise above the consensus range with further increases in force, attaining finally an absurdly large value, 92.4 nm at 3.9 pN. Moreover, no *uniform* scaling of z_F/z_{max} values, as would be required to correct for the use of a single incorrect z_{max} value, completely removes the force dependence of P_{app} or simultaneously elevates the too-small P_{app} values at low force and decreases the too-large values

DOI: 10.1021/acs.jpcb.5b03174
J. Phys. Chem. B XXXX, XXX, XXX–XXX

at high force into the consensus range. There is clearly some kind of problem with the relative extension data.

An alternative strategy, inspired by the X-ray scattering studies of Mathew-Fenn et al.[18] and Shi et al.,[19] is to assume that P = 50 nm at all forces but that the contour length varies with pulling force, as an equilibrium between a shorter and a longer conformation is progressively tilted toward the longer species by increasing force. In this interpretation, the *experimental* value, $(z_F/z_{max})_{ex}$, is still assumed to have been reckoned from the measured z_F using the same (unknown) value of z_{max} for all forces, but the left-hand side of the theoretical eq 2 must be modified to

$$z_F/L_F = (1 - (0.5)/(PF/kT - 1/32)^{1/2}) \quad (3)$$

where L_F is the appropriate contour length *for the force F*. After writing $z_F/L_F = (z_F/z_{max})(z_{max}/L_F)$, eq 3 is rearranged to give

$$L_F/z_{max} = (z_F/z_{max})_{ex}/(1 - (0.5)/(PF/kT - 1/32)^{1/2}) \quad (4)$$

For each force, the reported experimental $(z_F/z_{max})_{ex}$ value and an assumed value, P = 50 nm, are employed in eq 4 to determine the value of L_F/z_{max}. For each force, the ratio of the contour length L_F at force F to that at force 3.9 pN is reckoned according to $L_F/L_{3.9} = (L_F/z_{max})/(L_{3.9}/z_{max})$, and the resulting values are listed in Table 1.

The difference in average contour length per bp between a DNA held at force F and that held at 3.9 pN is given by

$$\Delta h_F \equiv h_F - h_{3.9} = (L_F/L_{3.9} - 1)h_{3.9} \quad (5)$$

where $h_F = L_F/N$ is the rise per bp at force F. We assume that $h_{3.9}$ = 0.338 nm, which is the value obtained by Marko and Siggia[24] from a two-parameter (L and P) global fit of their exact theory to the extension data reported by Smith et al.[29] for a 97004 bp DNA in 0.01 M ionic strength. Those data sampled a wide range of forces from ~0.028 to ~24.0 pN, particularly heavily at forces exceeding ~1.0 pN. Although $L_{3.9}$ at the higher ionic strength (~0.1 M) in the studies of Mosconi et al.[3] likely differs slightly from this value, the studies of Wang et al.[30] suggest that the contour length is moderately insensitive to ionic strength from 0.01 to 0.14 M. Values of Δh_F calculated by using $h_{3.9}$ = 0.338 nm in eq 5 are plotted vs F in Figure 2.

These data indicate that the rise per bp increases with increasing F (from 0.18 to 2.0 pN) before leveling off at higher forces. Such behavior suggests that a force-induced saturation of a structural transition between shorter and longer conformations may be taking place over this range of forces. The solid curve in Figure 2 results from the fit of a simple cooperative two-state model, as described in the next two sections.

The contour length at F = 0.18 pN is lower than that at 3.9 pN by only 0.93-fold, corresponding to a relative decrease of ~7%, whereas the intrinsic torsional rigidity at F = 0.25 pN is lower than that at 3.9 pN by ~0.55-fold, corresponding to a relative decrease of ~45%. The small relative size of the reduction in contour length with decreasing force could conceivably arise from some systematic force-dependent error in the relative extension measurements. Consequently, these Δh_F values are less robust than the much larger relative differences in torsional rigidity. Nevertheless, further analysis is merited for two reasons. (1) The coexistence of two (or more) conformations with slightly different contour lengths was inferred from X-ray scattering studies of short (10−35 bp) DNAs with attached gold colloids.[18,19] (2) That would provide a plausible mechanism for the force-induced structural change that is responsible for the increase in intrinsic torsional rigidity.

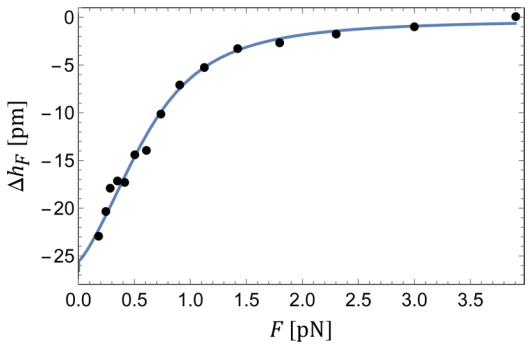

Figure 2. Difference in rise per bp ($\Delta h_F \equiv h_F - h_{3.9}$) vs pulling force ($F$). Experimental points are reckoned according to eq 5 from the $L_F/L_{3.9}$ values in Table 1, which were extracted from the data of Mosconi et al.[3] as described in the text. The solid line is a good fit (χ_r^2 = 0.93) of the two-state nearest-neighbor model embodied in eq 11 to these data with the following parameters: δ = 0.038 nm, $J^2 = 1.026 \times 10^{-5}$, B_0 = 0.997855, and p_0 = 1.007. The standard deviation, $\sigma_{\Delta h_F} \equiv 1 \times 10^{-12}$ m, was estimated semiquantitatively from the deviations of the experimental values from this smooth curve through the data.

THEORY AND FITTING PROTOCOLS

The Model for a Cooperative Two-State Stretching Transition. Each bp is assumed to exist in either of two states, a or b, which can interconvert, $a \rightleftharpoons b$. The rise per bp in state b exceeds that in state a by an amount, $\delta = h_b - h_a$, where by assumption h_b = 0.338 nm, and the values of δ and h_a remain to be determined. When F = 0, the free energy of state b relative to state a is $\Delta G^0 = G_b^0 - G_a^0 = -kT \ln B_0$, where B_0 is the intrinsic statistical weight of state b relative to that of state a, whose statistical weight is taken to be 1.0. When $F \neq 0$, the statistical weight of state b relative to state a becomes $B(F) = B_0 \exp[+F(z_F/L_F)\delta/kT]$, where the effective force acting to extend the DNA length is the average projection of F (directed along z) onto the DNA axis, namely, $F(z_F/L_F)$. In general, the statistical weight of state b is

$$B \equiv B(F) = B_0 \exp[+F\delta(1 - (0.5)/(PF/kT - 1/32)^{1/2})/kT] \quad (6)$$

which is evaluated using P = 50 nm and the adjustable values of B_0 and δ. The free energy (G_{alb}^0) of an unlike ($a|b$ or $b|a$) junction relative to that ($G_{a|a}^0 = 0 = G_{b|b}^0$) assigned to a like ($a|a$ or $b|b$) junction is $\Delta G_J^0 = G_{alb}^0 - 0 = -kT \ln J$, where J is the statistical weight of an unlike junction relative to a like junction.

The transfer matrix method[31] is employed with the matrix

$$\mathbf{M} = \begin{vmatrix} 1 & BJ \\ J & B \end{vmatrix} \quad (7)$$

The partition function is obtained by summing over all possible configurations (a or b) of all N bp's, and is given by

$$\chi = [1, b](M^{N-1})\begin{bmatrix} 1 \\ 1 \end{bmatrix} = [1, b]\mathbf{S}\begin{vmatrix} \lambda_+^{N-1} & 0 \\ 0 & \lambda_-^{N-1} \end{vmatrix}\mathbf{S}^{-1}\begin{bmatrix} 1 \\ 1 \end{bmatrix} \quad (8)$$

DOI: 10.1021/acs.jpcb.5b03174
J. Phys. Chem. B XXXX, XXX, XXX−XXX

Table 2. Fits of Theoretical Difference in Rise per bp Δh_F^{th} (eq 11) to Experimental Values Δh_F (eq 5)

fit	δ (nm)	B_0	J^2	$1 + 1/J$	P_0	$\chi_r^{2\,a}$	$f_b(0)$	$\langle h\rangle_0{}^b$ (nm)
(1)	0.0299	0.997095	5.155×10^{-6}	441	1.016	1.01	0.23	0.315
(2)	0.0380	0.997855	1.026×10^{-5}	313	1.007	0.93	0.34	0.313
(3)	0.0467	0.999283	2.012×10^{-5}	223	1.002	0.94	0.46	0.313

$^a\chi_r^2 = (1/(15-3))\sum_{j=1}^{15}(\Delta h_{F_j}^{th} - \Delta h_{F_j})^2/(\sigma_{\Delta h_F})^2$, wherein $\sigma_{\Delta h_F} = 1 \times 10^{-12}$ m, was estimated semi-quantitatively from deviations of the data from the fitted curve in Figure 2. $^b\langle h\rangle_0 = h_b - (1 - f_b(0))\delta$, wherein $h_b \equiv 0.338$ nm.

where λ_+ and λ_- are, respectively, the largest and smallest eigenvalues of **M** and **S** is the similarity transformation matrix that diagonalizes **M**. In the limit of large N, λ_-^{N-1} is so small compared to λ_+^{N-1} that it can be neglected, and all surviving terms contain the factor λ_+^N. In that case, $\ln \chi = N \ln \lambda_+ + Y$, where Y contains no terms that vary with N and consequently contributes negligibly to $\ln \chi$ in the large N limit. The eigenvalues of **M** are

$$\lambda_\pm = (0.5)(B + 1 \pm ((B-1)^2 + 4BJ^2)^{1/2}) \tag{9}$$

and the fraction of bp's in state b for force F is

$$\begin{aligned} f_b(F) &= (1/N)B\,\partial \ln \chi/\partial B \\ &= (B/\lambda_+)(\partial\lambda_+/\partial B) \\ &= (0.5)(1 + (B-1)/((B-1)^2 + 4BJ^2)^{1/2}) \end{aligned} \tag{10}$$

The theoretical expression for the average rise per bp at force F is taken to be $\langle h_F\rangle = f_a(F)h_a + f_b(F)h_b = f_b(F)\delta + h_a$, where $f_b(F)$ is reckoned for the appropriate force via eq 10. For the purpose of fitting the experimental Δh_F data, the *theoretical* difference between the average rise per bp at force F and that at $F = 3.9$ pN is taken to be

$$\Delta h_F^{th} = (f_b(F) - p_0) \tag{11}$$

where $f_b(F)$ is given by eq 10 and p_0 is an adjustable fraction in place of $f_b(3.9)$, and is employed for the following reason. The ideal *experimental* quantity desired is $\Delta h_F^I = h_F - h_{3.9}^{tr}$, where $h_{3.9}^{tr}$ denotes the hypothetical error-free true value at $F = 3.9$ pN. Experimental errors in h_F (or L_F) occur for all forces, including $F = 3.9$ pN. Consequently, it is generally expected that $\Delta h_{3.9}^I \neq 0$. Although Δh_F in eq 5 is the obvious approximation to Δh_F^I, it suffers the defect that $\Delta h_{3.9}$ is always forced to vanish, so any deviation of the experimental value, $h_{3.9}$, from the true value, $\Delta h_{3.9}^I$, cannot be taken into account. However, the use of an adjustable p_0 in eq 11 for fitting the experimental values of Δh_F allows $\Delta h_{3.9}^{th}$ to differ from 0 in such a way that errors in $\Delta h_{3.9}$ have the same weight as those in Δh_F for any other force.

Equation 11 with four parameters (B_0, δ, J, and p_0) was least-squares fitted to the experimental Δh_F values, which were reckoned according to eq 5 using $L_F/L_{3.9}$ values that were extracted from the data of Mosconi et al.[3] by using eq 4, and are presented in Table 1. The Mathematica FindFit (gradient-based) routine could find a local optimum, given sufficiently narrow ranges of the disposable parameters, but could not find a unique global optimum that was independent of the selected parameter ranges. The strategy adopted here was to restrict one of the parameters, specifically $\delta = h_a - h_b$, to one of five separate ranges of $\sim \pm 0.004$ nm about various "center" values, 0.020, 0.030, 0.040, 0.050, and 0.060 nm, and to manipulate the ranges of the other parameters so as to achieve a local best-fit with the smallest reduced chi-squared value (χ_r^2) for each choice of range center. The fitting for each range of δ produced only a modest deviation of the best-fit value of δ from its center. Good and statistically equivalent fits were obtained for δ-ranges centered at 0.030, 0.040, and 0.050 nm, and their resulting best-fit parameters, χ_r^2 values, and calculated values of the fraction, $f_b(0)$, of bp's in the longer b state *at zero force* are listed in Table 2.

The best-fits obtained for the δ-ranges centered at 0.020 and 0.060 nm exhibited χ_r^2 values more than twice as large, are consequently far less likely, and are not considered further here. These results strongly suggest that statistically equivalent fits could be obtained over the entire continuous range from $\delta = 0.030$ to 0.050 nm but not far outside of that.

The best-fit values of J, B_0, and p_0 evolve as δ is progressively changed. The range of best-fit δ values, 0.030−0.047 nm, corresponds to 9−14% of the assumed rise per bp of the extended b-state ($h_b = 0.338$ nm). However, the corresponding best-fit curves of Δh_F^{th} vs F for all three δ values in Table 2 are nearly identical (not shown) and exhibit an increase in rise per bp from ∼0.93 to ∼1.00 times h_b upon increasing the force from 0.18 to 3.9 pN. The average rises per bp at $F = 0$ are reckoned as $\langle h\rangle_0 = f_a(0)h_a + f_b(0)h_b = h_b - (1 - f_b(0))\delta$, and are presented in Table 2. The three best-fit models yielded nearly identical values of $\langle h\rangle_0$. The Δh_F vs F curve for the $\delta = 0.038$ nm model is displayed along with the experimental values in Figure 2. The fit is obviously rather good, as expected from its low value of χ_r^2. The $\langle h\rangle_0$ values in Table 2 depend primarily on the assumed value, $h_b = 0.338$ nm, of the longer b state, which is not precisely known at present.

Each of the three good fits of the cooperative two-state model to the experimental Δh_F values (cf. Table 2) yields a set of parameters from which the fraction of $f_b(F)$ of bp's in the b state at any force can be calculated using eqs 10 and 6. These fractions differ significantly for the three different choices of δ at low forces, although they all lie in the range $f_b(3.9) = 0.990 \pm 0.001$ at $F = 3.9$ pN.

The ultimate question is whether any or all of the cooperative two-state models that fit the Δh_F vs F data (derived from the zero twist data of Mosconi et al.) also provide a reasonable fit of the $1/\alpha_{MN}$ vs F data (derived from the data of both Mosconi et al. and Lipfert et al.) in Figure 1, simply by adjusting the torsion elastic constants of the a and b states. This will be addressed subsequently.

The immediate question is whether indications of similar force dependence of the contour length can be found in the data of Lipfert et al.,[4] who reported numerous measurements of extension vs force (z_F vs F) for their DNA at zero twist in its buffer (137 M NaCl, 2.7 mM KCl, 10 mM phosphate) over a wide range of forces from 0.01 to ∼30.0 pN (Figure 10 of their Supporting Information). Their data up to 5 pN were fitted by an extremely accurate approximation[32] to the exact solution for an inextensible wormlike coil (wlc) model in order to determine the best-fit persistence length, $P_{wlc} = 44$ nm, and contour length, $L_{wlc} = 2.7$ μm, both of which were assumed not to vary with force. Although the resulting best-fit curve (Figure

DOI: 10.1021/acs.jpcb.5b03174
J. Phys. Chem. B XXXX, XXX, XXX−XXX

10 of their Supporting Information) fits the data well at forces in the range 3−5 pN, it appears to significantly overestimate the extensions at forces in the range 0.2−1.0 pN, and then crosses over and underestimates the extensions in the range 0.01−0.04 pN. Could the poor fit over the range F = 0.25−1.0 pN be improved by adopting the consensus value P = 50 nm and employing the ratios $L_F/L_{3.9}$ in Table 1 to determine the force-dependent contour lengths, as was done here? As an example, for F = 3.9 pN, the extension is reckoned using their best-fit values, P_{wlc} = 44 nm and L_{wlc} = 2.7 μm, in eq 3 to obtain $z^{wlc}_{3.9}$ = 2.49 μm, which lies on their best-fit curve *in a region of good fit*, where the experimental extensions at the same force are distributed equally above and below this value. By using this value of $z^{wlc}_{3.9}$ and P = 50 nm in eq 3, one finds $L_{3.9}$ = 2.69 μm, which is very close to L_{wlc}, as expected. Now this $L_{3.9}$ is used with the ratio, $L_{0.25}/L_{3.9}$ = 0.94 in Table 1, to predict $L_{0.25}$ = 1.83 μm, which in turn is used along with P = 50 nm in eq 3 to obtain $z_{0.25}$ = 1.80 μm. This value can be compared with that reckoned by inserting P_{wlc} = 44 nm and L_{wlc} = 2.7 μm into eq 3 along with F = 0.025 pN to obtain $z^{wlc}_{0.25}$ = 1.88 μm. This latter value lies on the best-fit curve in a region of poor fit, where most of the data points for a given force lie toward lower extensions than that predicted by the wlc curve. However, the $z_{0.25}$ = 1.80 nm computed above is a somewhat lower extension, and appears to be much nearer the center of the extension data at that same force. From this example, it seems likely that a model with the consensus P = 50 nm and a force-dependent contour length similar to that manifested in the data of Mosconi et al. would provide a better overall fit of the z_F vs F data of Lipfert et al. over the entire region from 0.25 to 3.9 pN.

Self-interactions, which are omitted from the wlc theory, act to significantly enhance the coil extension at very low forces, and may contribute to the observed underestimation of the experimental extension by the best-fit wlc curve of Lipfert et al. in that region.

Comparable deviations of best-fit wlc theory from z vs F data are not observed for DNA in ∼0.01 M ionic strength buffer.[24,29] If a difference in behavior between DNAs in 0.1−0.15 M and in 0.01 M ionic strengths is confirmed by future studies, that might suggest that the larger electrostatic free energy in 0.01 M ionic strength is able to tilt the two-state equilibrium heavily toward the longer b state.

Can the Same Model Fit the Torsion Elastic Constant vs Force Data? When a total twist, θ (rad), is applied to the end of a chain of N identical springs with force-dependent intrinsic torsion elastic constant, α_F, and the chain axis is held stationary, the measured torque is $\tau = \alpha_F\theta/N = C^{in}_F\theta/L_F$, where $C^{in}_F = h_F\alpha_F$ is the force-dependent intrinsic torsional rigidity and $h_F = L_F/N$. From the measured torque, τ, one can obtain $\alpha_F = N\tau/\theta$ if N is known or $C^{in}_F = L_F\tau/\theta$ if L_F is known but N is not. When L_F declines with decreasing force, as appears to be the case in the studies of Mosconi et al. and Lipfert et al., then the use of a constant value, L_{wlc} (determined by fitting a wlc model to all of the data at different forces), in place of L_F is equivalent to using a constant value, $h_{wlc} = L_{wlc}/N$, in place of h_F to obtain the now slightly erroneous quantity, $\tilde{C}^{in}_F = (L_{wlc}/L_F)C^{in}_F = h_{wlc}\alpha_F$. At the higher forces, it is expected that $h_{wlc} \cong h_F$ and $\tilde{C}^{in}_F \cong C^{in}_F$, but at the lower forces $h_{wlc} > h_F$ and $\tilde{C}^{in}_F > C^{in}_F$. The tilde is used to indicate that the torsional rigidity, $\tilde{C}^{in}_F$, slightly exceeds the true value, C^{in}_F, for the lower values of F. This $\tilde{C}^{in}_F$ is the quantity determined by both Mosconi et al. and Lipfert et al. Nevertheless, $\tilde{C}^{in}_F$ preserves correctly the *relative* magnitudes of the α_F. The C^{in}_{MN} in Table 1 represent $\tilde{C}^{in}_F$ values, so $\alpha_{MN} \equiv C^{in}_{MN}/h_0 = (h_{wlc}/h_0)\alpha_F$, wherein h_0 = 0.338 nm is the consensus rise per bp, and h_{wlc} is unknown (since N is unknown) but independent of F and certainly rather close to h_0. Henceforth, we assume that $h_{wlc}/h_0 = 1.0$, so $\alpha_{MN} = \alpha_F$, and accept any small force-independent error resulting from that assumption. Thus, α_{MN} will be regarded as the experimental force-dependent intrinsic torsion elastic constant of the effective springs between bp's.

We now assume that the springs of bp's in the a and b states have constant intrinsic torsion elastic constants, α_a and α_b, respectively. For a DNA comprising two different kinds of springs, the measured intrinsic torsion elastic constant, α_{MN}, is *not* the weighted average of the two different elastic constants. Instead, $1/\alpha_{MN}$ is the weighted average of the two inverse torsion elastic constants. The theoretical mean inverse torsion elastic constant depends upon F, and is related to α_a and α_b by[33]

$$\langle 1/\alpha^{th}_F\rangle \equiv (f_a(F)/\alpha_a) + (f_b(F)/\alpha_b) \tag{12}$$

This $\langle 1/\alpha^{th}_F\rangle$ is fitted to the inverses of the α_{MN} in Table 1 by adjusting only α_a and α_b. The $f_b(F)$ were computed for each force via eqs 6 and 10 using one (or another) of the three best-fit sets of the parameters, δ, B_0, and J^2, in Table 2. The fit was biased in the sense that the parameter range for α_a was adjusted so that the computed curve of $\langle 1/\alpha^{th}_F\rangle$ passed visually close to the experimental points at F = 0.25 and 0.29 pN. Although this biasing did not attain the lowest possible value of χ_r^2, those values were still acceptably small. Lower χ_r^2 could be obtained only by allowing the curve to fall well below the data points at 0.25 and 0.29 pN and much closer to that at 0.50 pN. The biasing was tantamount to giving extra weight to fitting the two data points at 0.25 pN (Lipfert et al.) and 0.29 pN (Mosconi et al.), which is justified to some extent by the close mutual agreement of those values, and by the fact that both data sets exhibited a steep initial slope, which the actual best-fit curve captures much less well. This biased fitting protocol was performed for each of the three sets of best-fit parameters in Table 2, and the resulting values of α_a and α_b and χ_r^2 are listed in Table 3.

The curve from fit (2) is displayed in Figure 1. The visual quality of all three fitted curves (not shown) is very similar. These fitted curves provided a better visual fit to the $1/\alpha_{MN}$ values derived from the data of Lipfert et al. (large dots) than to those derived from the data of Mosconi et al. (small dots). In

Table 3. Fits of the Theoretical Inverse Torsion Elastic Constant $\langle(1/\alpha^{th}_F)\rangle$ (eq 12) to the Experimental $(1/\alpha_{MN})$ in Table 1

fit	$\alpha_a \times 10^{19}$ (J)	$\alpha_b \times 10^{19}$ (J)	$\chi_r^{2\,a}$	$\alpha_0 \times 10^{19}$ [b] (J)	$C^{in\,c}_0$ (fJ nm)	$\tilde{C}^{in\,d}_0$ (fJ nm)
(1)	5.44	11.98	1.14	6.22	196	210
(2)	4.81	12.05	1.00	6.05	189	204
(3)	4.13	12.05	0.94	5.92	185	200

[a] $\chi_r^2 = (1/(18-3))\sum_{j=1}^{18}(\langle 1/\alpha^{th}_F\rangle - 1/\alpha_{MN})^2/(\sigma_1/\alpha_{MN})^2$, where $\sigma_1/\alpha_{MN} = 1 \times 10^{17}$ J^{-1} was estimated semiquantitatively from the deviations of $1/\alpha_{MN}$ from the fitted curve in Figure 1. [b] Calculated as $1/(\langle(1/\alpha^{th}_F)\rangle)$, using eq 12 with F = 0. [c] Calculated using eq 13. [d] Calculated using eq 14.

DOI: 10.1021/acs.jpcb.5b03174
J. Phys. Chem. B XXXX, XXX, XXX−XXX

both cases, the present two-state model that fits the variation in contour length with F also gives (with suitable adjustment of α_a and α_b) a sufficiently good overall account of the somewhat imprecise $1/\alpha_{MN}$ data that it merits serious consideration as a rationalization of the unexpectedly large variation in C_{eff} with pulling force.

The predicted torsion elastic constants at zero force, α_0, are also listed in Table 3. The theoretical intrinsic torsional rigidity at zero force is given in each case by

$$C^{in}(0) = \alpha_0 \langle h \rangle_0 \tag{13}$$

where $\langle h \rangle_0$ is the average rise per bp at zero force in Table 2. As noted above, both experimental and theoretical α values contain a factor of h_{wlc}/h_0, which, if not 1.0, will necessitate a small correction of $C^{in}(0)$ by a constant factor near 1.0. In order to compare with the slightly erroneous experimental C^{in}_{MN} in Table 1, which takes no account of the length variation with force, one should probably use

$$\tilde{C}^{in}(0) = \alpha_0 h_0 \tag{14}$$

which simply restores the h_0 = 0.338 nm that was originally divided out of C^{in}_{MN} (to obtain the α_{MN} in Table 1). The $\tilde{C}^{in}(0)$ values for the different sets of model parameters are also listed in Table 3. The $C^{in}(0)$ takes into account the variation in rise per bp with force, whereas $\tilde{C}^{in}(0)$ does not. All of the $C^{in}(0)$ and $\tilde{C}^{in}(0)$ lie in the range measured by FPA for unstrained DNAs.

An Essential Flaw in the Present Analysis. The MN theory was employed to analyze experimental data for both the variation in rise per bp of an untwisted DNA and the variation of intrinsic torsional rigidity with force. However, that theory applies strictly only to filaments with uniform rise per bp and intrinsic torsional rigidity. We have *assumed* that the same theory applies as well, when the *average* rise per bp and *average* inverse torsional rigidity are used in place of the corresponding uniform values. It is implicitly assumed that local fluctuations in C^{in}_{MN} caused by fluctuations in tension, or equivalently orientation (about the average value), along the filament contribute negligibly to the average torque and C_{eff}. While this assumption is probably a reasonable approximation in a mean-projection overall sense, it must to some extent be wrong in quantitative detail. Specifically, a segment of n successive bp's in the longer b state will on average have a greater projection along the direction of the force than a segment of n successive bp's in the shorter a state, and this circumstance is not taken into account in the theory except in a preaveraged way. Consequently, some discrepancy between theory and experiment is to be expected. Nevertheless, it is likely that MN theory using the average $\langle h_F \rangle$ for the rise per bp and $\langle 1/\alpha_F \rangle^{-1}$ for the intrinsic torsion elastic constant will prove to be a reasonably good approximation to the eventual exact theory for this cooperative two-state model.

DISCUSSION

Best-Fit Parameters of the Two-State Model. *Rise per bp.* The range of acceptable values of the difference in rise per bp between the b and a conformers, δ = 0.030−0.047 nm, almost certainly extends sufficiently far at its low end to include also the value δ = 0.029 nm, which was extracted by Shi et al. from their X-ray scattering data.[19] In this respect, the results of the present analysis are consistent with those of Shi et al.[19]

Torsional Rigidity. The intrinsic torsion elastic constant of the b-state prevailing at the higher forces (≳4.0 pN) lies in the range $\alpha_b = (11.98-12.05) \times 10^{-19}$ J, which corresponds to an intrinsic torsional rigidity in the range C^{in}_b = 405−407 fJ fm, typical of DNAs subject to forces exceeding 4 pN. This also lies within the range of values, C^{in} = 310−420 fJ fm, measured for DNA circles containing N = 181−247 bp's by both topoisomer ratio and FPA methods but not for DNA circles containing $N \geq$ 340 bp's, where torsional rigidities in the range C^{in} = 170−231 fJ fm prevail.[7] Either sufficient tension or sufficient coherent bending strain can drive DNA in ∼0.1 M ionic strength at ∼293 K to structural states with comparably large torsional rigidities.

Addition of ethylene glycol (EG) at 310 K also induces an apparent two-state, cooperative, structural transition to an alternative state with an intrinsic torsional rigidity in the range C^{in} = 385−424 fJ fm.[31] However, the persistence length, $P \cong$ 30 nm at 310 K, and CD spectrum of the EG-induced state[31] are significantly smaller than the corresponding persistence lengths, P = 48−52 nm, and CD spectrum of the bending- and tension-induced states in 0.1 M ionic strength at 293 K. Although the alternative b state induced by tension is obviously not identical in all respects to those induced by bending strain or high concentrations of EG, its similarly high torsional rigidity is conceivably rooted in some common aspect of their structures, perhaps increased tilt of the base planes away from the normal to the helix-axis.

Large Cooperative Domain Sizes. The average domain size at the midpoint of the tension-induced transition is $\langle n_J \rangle = 1 + 1/J$,[31] and in Table 2 ranges from 441 to 223 bp's, as the best-fit δ ranges from 0.030 to 0.047 nm. The high cooperativity implied by such large domain sizes enables weak forces in the range F = 0.25−1.0 pN to substantially shift the prevailing equilibrium between the shorter and longer conformations. The difference in extension between a *mean domain* of b and a *mean domain* of a is the relevant "handle" by which the pulling force tilts the $a \rightleftharpoons b$ equilibrium near the midpoint of the transition.

Prior Evidence of Large Domains of Alternative Structure. Evidence of large-domain structural transitions in dilute DNA molecules at ambient temperature was first reported in 1984.[10,11,14] Extensive secondary structure switching in native supercoiled circular DNAs in 10−15 mM ionic strength at 293 K was serendipitously observed upon changing the buffer from Tris to citrate (a strong Mg^{2+} chelator), or upon releasing negative superhelical strain by linearization with a restriction enzyme,[10,11] and later also upon increasing negative superhelical strain by removing bound ethidium from circular DNAs that had been previously relaxed by topoisomerase I in the presence of various concentrations of ethidium.[34] The extensive, if not global, nature of the switching was inferred from (1) the surprisingly large *relative* changes in both torsion elastic constants (determined by FPA) and circular dichroism (CD) spectra and (2) the appearance of long-lived (several weeks) metastable secondary structure with anomalously low torsion elastic constant immediately after release of superhelical strain.[10,11] Such long-lived metastable secondary structure was later also observed in DNAs in 0.1 M ionic strength subsequent to relaxation of superhelical strain by linearization,[10,11] binding of *E. coli* single-strand binding protein,[11,35] binding various intercalators that unwind the DNA,[11,36,37] and by the action of topoisomerase I, which also was recently shown to catalyze the eventual equilibration of the initially formed metastable secondary structure.[38] The inability of a large fraction of the

DOI: 10.1021/acs.jpcb.5b03174
J. Phys. Chem. B XXXX, XXX, XXX−XXX

newly relaxed DNA to revert immediately to the equilibrated normal secondary structure of the unstrained DNA necessarily implies that a comparable (or larger) fraction of the supercoiled DNA must have exhibited one or more alternative secondary structures that were originally induced by its superhelical strain.

A high degree of cooperativity was qualitatively suggested by (1) the apparent abruptness of the induced transitions[11,34] and (2) the uniformity of the torsion elastic constant over distances up to 200 bp's on either side of the ethidium probe, even during periods when the torsion elastic constant was evolving slowly over time. This uniformity could be inferred from the close similarity of the best-fit α values obtained by fitting the FPA data over different time-spans (0−18, 0−35, 0−70, and 0−120 ns).[10,11] The FPA measurement is sensitive to dynamic twisting correlations between the probe dye and its surrounding base pairs. Such correlations extend over increasingly greater distances from the probe with increasing time span of the experiment up to ∼200 bp's at 120 ns.[39] The absence of such variations in α with time span argues that the ethidium probe was sampling domains of such large size, that it was rarely within 200 bp's of a boundary between domains of significantly different torsional rigidity. Such large domains are the hallmark of a highly cooperative structural transition. The ultraslow kinetics of equilibration subsequent to certain changes in superhelical strain are also consistent with a highly cooperative transition, since the nucleation step of such a process is extremely slow. The possible role of highly cooperative allosteric transitions in supercoiled DNAs to facilitate long-range signaling between two proteins bound to well-separated specific sites was introduced and discussed, and a specific example was analyzed.[10]

Long-Range Allosteric Transitions Induced by Local Perturbations. Highly cooperative structural transitions could be induced also in certain linear DNAs in 0.1 M ionic strength by particular *local* structural perturbations. Replacing 26 bp's of the native sequence by a 16 bp $(CG)_8$ sequence near the middle of an ∼1100 bp subfragment of p30δ DNA caused an ∼0.75-fold reduction in α, a 1.3-fold increase in the maximum molar ellipticity near 273 nm ($[\theta]_{273}$), and an increase in the susceptibility to S1 nuclease attack, which appeared to be altered over the entire length of the 1097 bp DNA.[14,40] Such relative changes are so disproportionately large compared to the tiny fraction (0.024) of altered sequence that they cannot be rationalized by assigning any plausible values of α, $[\Theta]_{273}$, or S1 susceptibility solely to the $(CG)_8$ sequence. By setting a plausible lower limit for α ($0.5 \times \alpha$ of control DNA) and a plausible upper limit for $[\theta]_{273}$ ($2.0 \times [\theta]_{273}$ of control DNA) of the altered state of the DNA flanking the $(CG)_8$ insert, lower bounds of 330 and 550 bp's, respectively, were estimated for the domain size of the altered DNA, and there was no evidence (e.g., from S1 cutting) to suggest that altered secondary structure did not extend over the entire molecule.[14,40] Raising the NaCl concentration above 2.5 M, which presumably induced a B → Z transition of the $(CG)_8$ sequence, induced another long-range (or large domain) transition of the flanking DNA to a state of greater dynamic bending rigidity.[14,40] Adding 1 ethidum per 300 bp's to the same DNA in 4.3 M NaCl induced a third long-range structural transition of the flanking DNA to a state with a substantially reduced bending rigidity and a doubled $[\theta]_{273}$.[14,40] Control DNAs without the $(CG)_8$ insert sequence showed none of these transitions.[14,40] Metastability and ultraslow (>several days) kinetics accompanied the transitions induced by increasing salt concentration and ethidium binding in 4.3 M NaCl. After removing the ethidium and returning the salt concentration to 0.1 M by dialysis, the original properties of the inset fragment were eventually recovered, so these transitions were reversible in that sense. Circular dichroism spectra strongly suggested that all structures exhibited by DNA flanking the $(CG)_8$ insert were within the B-family. These experiments and others described in the original paper[40] established unequivocally that local perturbations of a pure (uncontaminated by proteins or polyamines), intact (without single-strand breaks), completely sequenced, isolated (nonassociated), normal (in regard to gel mobility, sedimentation coefficient, and friction factor) duplex DNA can induce highly cooperative long-range structural transitions of the flanking DNA that extend over domains of *at least* a few hundred bp's, and that the induced structures most likely lie within the B-family. These and other examples of the striking long-range effects of $(GC)_n$ inserts on their flanking DNA were reviewed.[14]

Binding of a tetramer of the Sp1 transcriptional activator to its consensus binding site near the middle of a 1074 bp linear DNA (in ∼0.075 M ionic strength plus 20% glycerol) converted the circular dichroism spectrum from that of canonical B(10.4) DNA almost completely to the partially inverted spectrum typical of B(10.2) DNA.[14] In addition, the effective ethidium binding constant was reduced by a factor of 6, which requires conversion of *at least* 5/6 of the total sequence (914 bp's) to the altered (B(10.2)) state, which evidently has a far lower affinity for ethidium. Increasing the amount of ethidium by 2.5-fold (from 1/250 to 1/100 bp) increased the effective ethidium *binding constant* by 2.25-fold, indicating that some (∼212 bp's) of the altered (B(10.2)) structure had been switched back to its original B(10.4) structure. The apparent torsional rigidity of this DNA with 1 added ethidium/250 bp's was enhanced in the presence of Sp1 by 1.4-fold above that in the absence of Sp1. However, this might be only a lower bound to the actual enhancement, because clustering of the ethidium probes on the unaltered DNA near the ends of the filament might promote significant excess depolarization due to excitation transfer,[37] which would diminish the apparent α. In addition, such probes would experience only the greater amplitudes of torsional motion near the filament ends, which also would lower the α value obtained from the FPA data by the standard fitting protocol, which is predicated on random positioning of the ethidium probes over the entire length of the DNA. This study provided perhaps the strongest evidence to date for a very long-range allosteric transition of DNA induced by the binding of a transcriptional activator to a linear DNA, although in this example, its effect is inhibition, rather than enhancement, of ethidium binding out to a distance of several hundred bp's on either side of the binding site.[14]

Evidence suggesting that very long-range allosteric transitions are induced in supercoiled DNAs by (i) site-specific binding of dimers of CAP·cAMP (complex of catabolite activator protein with cyclic adenosine monophosphate) and by the binding of IHF (integration host factor) protein, both of which can function as transcriptional activators, has been reported and reviewed.[14,41,42] In the latter case, a detailed analysis[14] indicated that the originally proposed[42] superhelical strain redistribution mechanism could not account for many of the experimental data, especially those in the 110−158 mM (or higher) ionic strength range, where superhelix densities in the range $\sigma = 0$ to −0.05 do *not* give rise to stably melted regions at 37 °C.[43]

DOI: 10.1021/acs.jpcb.5b03174
J. Phys. Chem. B XXXX, XXX, XXX−XXX

Much of the evidence points to a direct long-range allosteric transition induced by the IHF binding as the primary mechanism, at least in 110−158 mM ionic strength, with supercoiling providing a more or less independent secondary contribution.[14]

When m bp's in a hypothetical uniform DNA that exhibits a cooperative two-state equilibrium are fixed in one of those two states, the probability that they are followed by a run of n consecutive unconstrained bp's in the same state before encountering the first unconstrained bp in the other state decays exponentially with increasing n. When the two states have the same statistical weight, the average length of such runs is $1/J$ bp. Such cooperative domains are expected on either side of the m constrained bp, yielding an average total domain size of $m + 2/J$ bp, which would be expected to be equal to or exceed 447−882 bp's for the models that best fit the present force-induced transition. Such large domain sizes are in the range of some of those induced by local structural perturbations in linear DNAs that were discussed above.

Highly Cooperative Structure Switching Requires B_0 close to 1.0. The present model is capable of fitting the data only over an extremely narrow range of B_0 values near 1.0. This circumstance arises because very great cooperativity (meaning very small J) is required to significantly shift the two-state equilibrium over the range of pulling forces involved. For a given very small cooperativity parameter, J, only B_0 values very close to 1.0 allow a reasonable fit of this simple two-state model to the experimental extension vs force data. In general, a highly cooperative allosteric transition, $a \rightarrow b$, could have a very different initial relative statistical weight, B_0, of the b and a states and the transition induced by increasing pulling force (or other perturbation) would be very abrupt, when it finally occurs. The problem in the present example is that, in order for a transition to be induced over the range of forces, 0.25−1.0 pN, either B_0 has to be nearly 1.0, or δ would have to be unphysically large and far greater than the value reported by Shi et al.[17]

Comment on the Two-State Model. The two-state nearest-neighbor interaction model is the very simplest approximation to more realistic multistate multineighbor interaction models that also exhibit two distinct minimum free energy (or minimum potential of mean force) regions in the selected coordinate space used to define the structure(s) of the a and b states at the desired level of resolution. Hence, the best-fit parameters of the two-state nearest-neighbor model should be interpreted cautiously, because they likely contain contributions from multiple parameters of rather more complex underlying models.

Cooperative Bistable Allostery vs Simple Strain Propagation. According to current understanding,[44] allostery requires the following:

(1) The existence of two distinct minima in the potential of mean force as a function of the relevant coordinates that define the structure at any single functional "site", which in the case of DNA could be an RNA polymerase binding sequence.
(2) A sensitivity of functional processes, such as RNA polymerase binding, at the functional site to the prevailing minimum potential-of-mean-force structure at that site.
(3) A separate binding site (for an allosteric activator), the occupation of which induces a structural change that alters the relative stabilities of the two potential-of-mean-force minima at the functional site, and thereby enables a subsequent *shift of population* between them. Such activator binding effectively flips a bistable switch in the level of function at the functional site. The kinetics of the population shift is necessarily hindered by the barrier between the two (or more) minima in the potential of mean force at the functional site, which in extreme cases can lead to metastability and hysteresis of the switching process.

The present cooperative two-state nearest-neighbor interaction model in principal satisfies the criteria for allosteric control of DNA structure at a functional site (subsequence), which could work in the following way(s). Suppose an allosteric activator protein either binds more strongly to the b state than to the a state of its cognate sequence or substantially lowers the free energy to form an $a|b$ or $b|a$ junction within its binding site. Binding this protein to its cognate sequence would then enhance the population of b structure at the separate (but not too distant) functional site, and thereby facilitate binding of a functional protein that similarly prefers the b state to the a state at is cognate sequence.

True allostery like that just described is not the only means by which binding a ligand, L1, at one site can affect binding of a second ligand, L2, at a functional site in the vicinity. For any three-dimensional solid object with finite elasticity, the imposition of local strain over some subset of atoms occupying a well-defined subvolume will inevitably also introduce strain into adjacent regions beyond the boundaries of that deformed subvolume. This strain "propagation" normally dies out gradually over relatively short distances beyond the boundary of the deformed subvolume. For example, in normal DNA, the strain accompanying the extension and unwinding caused by intercalation of ethidium or chloroquine extends beyond the first bounding bp's on either side so as to preclude intercalator binding at its nearest-neighboring intercalation sites but has no apparent influence on any intercalation sites beyond that. Consequently, ethidium and chloroquine binding follow the well-known nearest-neighbor exclusion model (cf. refs 22, 36, 37, and 45 and references contained therein). However, other kinds of local strain, namely, widening the major groove or pulling the two strands slightly apart, which are to some extent equivalent, apparently propagate along the helix in an exponentially damped oscillatory manner with a decay length of 10−15 bp's and a 10 bp period.[46,47] In fact, binding of a protein (designated as P2 here) with a strong affinity for a wide major groove at its cognate sequence (site 2) was observed to modulate the binding of a second protein (designated as P1 here), with a similar preference for a wide major groove at its own cognate sequence (site 1), and the modulation amplitude exhibited damped (decay length ∼15 bp's) oscillations (∼10 bp's) with increasing separation between the two sites.[46] Because only a *single* minimum free energy (potential-of-mean-force) structure prevails at site 1, either in the naked DNA, or when P2 is bound to site 2 (which induces a single deformed structure at site 1), there should be no free energetic barrier to population shift between two or more prevailing minima in this case. Hence, the kinetics of relaxation of the altered DNA structure at an empty P1 site after removal of P2 should be extremely rapid (sub-nanosecond strain release) with no sign of metastability or hysteresis. Although modulation of structure and function at a functional site simply by propagating strain

DOI: 10.1021/acs.jpcb.5b03174
J. Phys. Chem. B XXXX, XXX, XXX−XXX

from a nearby perturbed site does not constitute true allostery, as currently understood,[44] it is conceivably as important (or more so) in gene regulation. However, the range of signal transmission is almost certainly far smaller than what is potentially achievable with highly cooperative models involving two (or more) distinct potential-of-mean-force structures with comparable stability at the active site.

Other Evidence for Coexistence of Alternative Structures over the Same Sequence of DNA under the Same Conditions. The dynamic bending rigidity of DNA, which governs its Brownian flexural dynamics on short time scales, $t < 1\ \mu s$, exceeds by 3- to 4-fold the apparent equilibrium bending rigidity determined from its equilibrium persistence length, which reflects its rms curvature and contains contributions of permanent bends and slowly relaxing bends in addition to dynamic bends.[15,48] This observation cannot be rationalized without invoking a kinetically slow ($t > 10\ \mu s$) transition between two (or more) differently curved secondary conformations over a significant fraction of the sequence.

The coexistence of two slightly different structures of the same duplex DNA molecule with the sequence 5′-CCAGGCC-TGG-3′ in the *same* crystal provides irrefutable evidence of bistability involving two distinct minima in the potential of mean force for the coordinates that define these structures.[49] The two central bp's, and most of the backbone atoms, hydrated Mg^{2+} ions, and proximal water molecules are found in either of two main distinct structures. Preliminary examination of the reported high-resolution diffraction structures for other DNA molecules suggests that multiple coexisting structures in DNA crystals may be rather more common than previously thought.[49]

Comparison of RNA and DNA. Similar experiments to those of Lipfert et al.[4] described above were also performed on a 4.2 kbp duplex RNA with rather similar results.[50] In particular, the effective torsional rigidity declines with decreasing force below ∼2.0 pN to values substantially below the predictions of MN theory for an appropriate value of the intrinsic torsional rigidity, which was chosen to match the theory to experiment at a force of ∼6.5 pN. The apparently broader transition zone (of C^{eff} vs F) for RNA might reflect a somewhat lower cooperativity of the structural transition in that case. A careful analysis of relative extension vs force data for untwisted RNA over the range from 0.25 to 4.0 pN will be a prerequisite for analysis of the C^{eff} vs F data. That is a topic for future work.

Final Comment. Although the existence and properties of the present best-fit two-state nearest-neighbor model(s) of a force-induced structural transition in the low-force regime may seem bizarre to workers unfamiliar with the DNA literature beyond single molecule pulling experiments, they are in fact entirely consistent with properties of DNA that have been directly established by, or inferred from, a great many previous and contemporary experiments and data analyses. In the event that the apparent force-induced variation in length actually arises from a small systematic error in the experimental data of Mosconi et al., the present two-state nearest neighbor model and its best-fit parameters would be rendered meaningless, but the conclusion that the intrinsic torsional rigidity increases almost 2-fold with increasing force from 0.25 to 2.0 pN would still remain.

AUTHOR INFORMATION

Corresponding Author

*E-mail: jmschurr@zipcon.com. Phone: 206 522 7583.

Notes

The authors declare no competing financial interest.

ACKNOWLEDGMENTS

The author is grateful to Drs. Phil Nelson, Pehr Harbury, Rhiju Das, Xuesong Shi, Jan Lipfert, David Bensimon, and Alex Vologodskii for sharing their knowledge and insights, and to an anonymous reviewer for informative and helpful comments.

REFERENCES

(1) Moroz, J. D.; Nelson, P. Torsional Directed Walks, Entropic Elasticity, and DNA Twist Stiffness. *Proc. Natl. Sci. U.S.A.* **1997**, *94*, 14418−14422.
(2) Moroz, J. D.; Nelson, P. Entropic Elasticity of Twist-Storing Polymers. *Macromolecules* **1998**, *31*, 6333−6347.
(3) Mosconi, F.; Allemand, J. F.; Bensimon, D.; Croquette, V. Measurement of the Torque on a Single Stretched and Twisted DNA Using Magnetic Tweezers. *Phys. Rev. Lett.* **2009**, *102*, 078301−078304.
(4) Lipfert, J.; Kerssemakers, W. J.; Jager, T.; Dekker, N. H. Magnetic Torque Tweezers: Measuring Torsional Stiffness in DNA and RecA-DNA Filaments. *Nat. Methods* **2010**, *7*, 977−980.
(5) Bryant, Z.; Stone, M. D.; Gore, J.; Smith, S. B.; Cozzarelli, N. R.; Bustamante, C. Structural Transitions and Elasticity from Torque Measurements on DNA. *Nature* **2003**, *424*, 338−341.
(6) Lipfert, J.; Wiggin, M.; Kerssemakers, J. W. J.; Pedaci, F.; Dekker, N. H. Freely Orbiting Magnetic Tweezers to Directly Monitor Changes in the Twist of Nucleic Acids. *Nat. Commun.* **2011**, *2*, 439.
(7) Fujimoto, B. S.; Schurr, J. M. Torsional Rigidities of Weakly Strained DNAs. *Biophys. J.* **2006**, *91*, 4166−4179.
(8) Thomas, J. C.; Allison, S. A.; Appellof, C. J.; Schurr, J. M. Torsion Dynamics and Depolarization of Fluorescence of Linear Macromolecules. II. Fluorescence Polarization Anisotropy Measurements on a Clean Viral Φ29 DNA. *Biophys. Chem.* **1980**, *12*, 177−188.
(9) Thomas, J. C.; Schurr, J. M. Fluorescence Depolarization and Temperature Dependence of the Torsion Elastic Constant of Linear Φ29 DNA. *Biochemistry* **1984**, *22*, 6194−6198.
(10) Shibata, J. H.; Wilcoxon, J.; Schurr, J. M.; Knauf, V. Structures and Dynamics of a Supercoiled DNA. *Biochemistry* **1984**, *23*, 1188−1194.
(11) Schurr, J. M.; Fujimoto, B. S.; Wu, P.-G; Song, L. Fluorescence Studies of Nucleic Acids: Dynamics, Rigidities, and Structures. In *Topics in Fluorescence Spectroscopy, Vol. 3, Biochemical Applications*; Lakowicz, J. R., Ed.; Plenum Press: New York, 1992; pp 137−229.
(12) Fujimoto, B. S.; Schurr, J. M. Dependence of the Torsional Rigidity of DNA on Base Composition. *Nature* **1990**, *344*, 175−178.
(13) Heath, P. J.; Clendenning, J. B.; Fujimoto, B. S.; Schurr, J. M. Effect of Bending Strain on the Torsion Elastic Constant of DNA. *J. Mol. Biol.* **1996**, *260*, 718−730.
(14) Schurr, J. M.; Delrow, J. J.; Fujimoto, B. S.; Benight, A. S. The Question of Long-Range Allosteric Transitions in DNA. *Biopolymers* **1997**, *44*, 283−308.
(15) Naimushin, A. N.; Fujimoto, B. S.; Schurr, J. M. Dynamic Bending Rigidity of a 200-bp DNA in 4 mM Ionic Strength: A Transient Polarization Grating Study. *Biophys. J.* **2000**, *78*, 1498−1518.
(16) Heath, P. J.; Gebe, J. A.; Allison, S. A.; Schurr, J. M. Comparison of Analytical Theory with Brownian Dynamics Simulations for Small Linear and Circular DNAs. *Macromolecules* **1996**, *29*, 3583−3596.
(17) Chou, F.-C.; Lipfert, J.; Das, R. Blind Predictions of DNA and RNA Tweezers Experiments with Force and Torque. *PLoS Comput. Biol.* **2014**, *10*, e10037566.
(18) Mathew-Fenn, R. S.; Das, R.; Harbury, P. A. B. Remeasuring the Double-Helix. *Science* **2008**, *322*, 446−449.
(19) Shi, X.; Herschlag, D.; Harbury, P. A. Structural Ensemble and Microscopic Elasticity of Freely Diffusing DNA by Direct Measurement of Fluctuations. *Proc. Natl. Acad. Sci. U.S.A.* **2013**, *110*, E1444−E1451.

DOI: 10.1021/acs.jpcb.5b03174
J. Phys. Chem. B XXXX, XXX, XXX−XXX

(20) Horowitz, D. S.; Wang, J. C. Torsional Rigidity of DNA and Length Dependence of the Free Energy of DNA Supercoiling. *J. Mol. Biol.* **1984**, *173*, 75−91.
(21) Shore, D.; Baldwin, R. L. Energetics of DNA Twisting. II. Topoisomer Analysis. *J. Mol. Biol.* **1983**, *170*, 983−1007.
(22) Clendenning, J. B.; Schurr, J. M. Circularization of Small DNAs in the Presence of Ethidium, a Theoretical Analysis. *Biopolymers* **1994**, *34*, 849−868.
(23) Taylor, W. H.; Hagerman, P. J. Application of the Method of Phage T4 Ligase-catalyzed Ring-Closure to the Study of DNA Structure. II. NaCl −Dependence of DNA Flexibility and Helical Repeat. *J. Mol. Biol.* **1990**, *212*, 363−376.
(24) Marko, J. F.; Siggia, E. D. Stretching DNA. *Macromolecules* **1995**, *28*, 8759−8770.
(25) Baumann, C. G.; Smith, S. B.; Bloomfield, V. A.; Bustamante, C. Ionic Effects on the Elasticity of Single DNA Molecules. *Proc. Natl. Acad. Sci. U.S.A.* **1997**, *94*, 6185−6190.
(26) Geggier, S.; Kotlyar, A.; Vologodskii, A. Temperature Dependence of DNA Persistence Length. *Nucleic Acids Res.* **2011**, *39*, 1419−1426.
(27) Wenner, J. R.; Williams, M. C.; Rouzina, I.; Bloomfield, V. A. Salt Dependence of the Elasticity and Overstretching Transition of Single DNA Molecules. *Biophys. J.* **2002**, *82*, 3160−3169.
(28) Herrero-Galán, E.; Fuentes-Perez, M. E.; Carrasco, C.; Valpuesta, J. M.; Carrascosa, J. L.; Moreno-Herrero, F.; Arias-Gonzalez, J. R. Mechanical Identities of RNA and DNA Double Helices Unveiled at the Single Molecule Level. *J. Am. Chem. Soc.* **2013**, *135*, 122−131.
(29) Smith, S. B.; Finzi, L.; Bustamante, C. Direct Mechanical Measurements of the Elasticity of Single DNA Molecules by Using Magnetic Beads. *Science* **1992**, *258*, 1122−1126.
(30) Wang, M. D.; Yih, H.; Landick, R.; Gelles, J.; Block, S. M. Stretching DNA with Optical Tweezers. *Biophys. J.* **1997**, *72*, 1335−1346.
(31) Brewood, G. P.; Aliwarga, T.; Schurr, J. M. A Structural Transition in Duplex DNA Induced by Ethylene Glycol. *J. Phys. Chem. B* **2008**, *112*, 13367−13380.
(32) Bouchiat, C.; Wang, M. D.; Allemand, J.-F.; Strick, T.; Block, S. M.; Croquette, V. Estimating the Persistence Length of a Worm-Like Chain Molecule from Force-Extension Measurements. *Biophys. J.* **1999**, *76*, 409−413.
(33) Wilcoxon, J.; Schurr, J. M. Temperature Dependence of the Dynamic Light Scattering of Linear Φ29 DNA: Implications for Spontaneous Opening of the Double-Helix. *Biopolymers* **1983**, *22*, 2273−2321.
(34) Song, L.; Fujimoto, B. S.; Wu, P.-G.; Thomas, J. C.; Shibata, J. H.; Schurr, J. M. Evidence for Allosteric Transitions in Secondary Structure Induced by Superhelical Stress. *J. Mol. Biol.* **1990**, *214*, 307−326.
(35) Langowski, J.; Benight, A. S.; Fujimoto, B. S.; Schurr, J. M.; Schomburg, U. Change of Conformation and Internal Dynamics of Supercoiled DNA upon Binding *E. coli* Single-Strand Binding Protein. *Biochemistry* **1985**, *24*, 4022−4028.
(36) Wu, P.-G.; Song, L.; Clendenning, J. B.; Fujimoto, B. S.; Benight, A. S.; Schurr, J. M. Interaction of Chloroquine with Linear and Supercoiled DNAs. Effect on the Torsional Dynamics, Rigidity, and Twist Energy Parameter. *Biochemistry* **1988**, *27*, 8128−8144.
(37) Wu, P.-G.; Fujimoto, B. S.; Song, L.; Schurr, J. M. Effect of Ethidium on the Torsion Constants of Linear and Supercoiled DNAs. *Biophys. Chem.* **1991**, *41*, 217−236.
(38) Brewood, G. P.; Delrow, J. J.; Schurr, J. M. Calf-Thymus topoisomerase I Equilibrates Metastable Secondary Structure Subsequent to Relaxation of Superhelical Stress. *Biochemistry* **2010**, *49*, 3367−3380.
(39) Schurr, J. M.; Fujimoto, B. S. Dynamic Twisting Correlations in a Model DNA with Uniform Torsion Elastic Constant. *Biopolymers* **1999**, *49*, 355−359.
(40) Kim, U.-S.; Fujimoto, B. S.; Furlong, C. E.; Sundstrom, J. A.; Humbert, R.; Teller, D. C.; Schurr, J. M. Dynamics and Structures of DNA: Long-Range Effects of a 16 Base-Pair $(CG)_8$ Sequence on Secondary Structure. *Biopolymers* **1993**, *33*, 1725−1745.
(41) Parekh, B. S.; Hatfield, G. W. Transcriptional Activation by Protein-induced DNA Bending: Evidence for a DNA Structural Transmission Model. *Proc. Natl. Acad. Sci. U.S.A.* **1996**, *93*, 1173−1177.
(42) Parekh, B. S.; Sheridan, S. D.; Hatfield, G. W. Activation of Gene Expression by a Novel DNA Structural Transmission Mechanism that Requires Supercoiling-Induced DNA Duplex Destabilization in an Upstream Activating Sequence. *J. Biol. Chem.* **1998**, *273*, 21298−21308.
(43) Kowalski, D.; Natale, D. A.; Eddy, M. J. Stable DNA Unwinding, not "Breathing", Accounts for Single-Strand-Specific Nuclease Hypersensitivity of Specific A+T-Rich Sequences. *Proc. Natl. Acad. Sci. U.S.A.* **1988**, *85*, 9464−9468.
(44) Tsai, C.-J.; Nussinov, R. A. Unified View of How "Allostery Works. *PLoS Comput. Biol.* **2014**, *10*, e1003394.
(45) Clendenning, J. B.; Naimushin, A. N.; Fujimoto, B. S.; Stewart, D. S.; Schurr, J. M. Effect of Ethidium Binding and Superhelix Density on the Superhelix Density on the Supercoiling Free Energy and Torsion and Bending Constants of p30δ DNA. *Biophys. Chem.* **1994**, *52*, 191−218.
(46) Kim, S.; Broströmer, E.; Xing, D.; Jin, J.; Chong, S.; Ge, H.; Wang, S.; Gu, C.; Yang, L.; Gao, Y.-Q.; Su, X.-D.; Sun, Y.; Xie, X. S. Probing Allostery through DNA. *Science* **2013**, *339*, 816−819.
(47) Xu, X.; Ge, H.; Gao, Y. Q.; Wang, S. S.; Thio, B. J.; Hynes, J. T.; Xie, S.; Cao, J. Modeling Spatial Correlation of DNA Deformation: DNA Allostery in Protein Binding. *J. Phys. Chem. B* **2013**, *117*, 13378−13387.
(48) Okonogi, T.; Reese, A.; Alley, S. C.; Hopkins, P. B.; Robinson, B. H. Flexibility of Duplex DNA on the Sub-Microsecond Timescale. *Biophys. J.* **1999**, *77*, 3256−3276.
(49) Maehigashi, T.; Hsiao, C.; Woods, K. K.; Moulaei, T.; Hud, N. V.; Williams, L. D. B-DNA Structure is Intrinsically Polymorphic: even at the Level of Base Pair Positions. *Nucleic Acids Res.* **2012**, *40*, 3714−3722.
(50) Lipfert, J.; Skinner, G. M.; Keegstra, J. M.; Hensgens, T.; Jager, T.; Dulin, D.; Köber, M.; Yu, Z.; Donkers, S. P.; Chou, F.-C.; Das, R.; Dekker, N. H. Double-Stranded RNA under Force and Torque: Similarities to and Striking Differences from Double-Stranded DNA. *Proc. Natl. Acad. Sci. U.S.A.* **2014**, *111*, 15408−15413.

DOI: 10.1021/acs.jpcb.5b03174
J. Phys. Chem. B XXXX, XXX, XXX−XXX